Ind. Jour. Mech. Cont. & Math. Sci., Vol.1 July (2006) Pages 1-15

NUMERICAL STUDY OF PULSATILE MHD NON-NEWTONIAN FLUID FLOW WITH HEAT AND MASS TRANSFER THROUGH A POROUS MEDIUM BETWEEN TWO PERMEABLE PARALLEL PLATES

Mokhtar A. Abd Elnaby, Nabil T. M. Eldabe and Mohammed Y. Abou zeid
Department of Mathematics, Faculty of Education, Ain Shams University, Heliopolis, Cairo, Egypt.

(Received on February 1,2006)

Abstract

A Runge-Kutta-Merson method and a Newton iteration in a shooting and matching technique are used to obtain the solutions of the governing equations. These equations resulted from the unsteady motion of the magneto-hydrodynamic biviscosity fluid with heat and mass transfer through a uniform porous medium between two permeable parallel walls, taking into account pulsation of the pressure gradient. The velocity, temperature and concentration distributions are obtained as a perturbation technique. During this work we calculate an estimation of the global error by using Zadunaisky technique. The effects of upper limit of apparent viscosity coefficient, Reynolds number, permeability parameter, Forschheimer number, magnetic parameter, the steady component of the pressure gradient, the amplitude of the pulsation, Prandtl number, Eckert number, Schmidt number, Soret number and the time on the velocities, temperature and concentration distributions are evaluated and depicted graphically.

Keyword and phrases : *non-Newtonian fluid, heat transfer, mass transfer, plates.*

সংক্ষিপ্তসার

নিয়ন্ত্রক সমীকরণগুলির সমাধান নির্ণয় করতে রুঙ্গো-কুটা-মেসন পদ্ধতি এবং সুটিং ও সমবাক্ষ বস্তুর ক্ষেত্রে নিউটন পুনরাবৃত্তিকার কৃৎকৌশল প্রয়োগ করা হয়েছে। স্পন্দনের চাপের নতিকে হিসা-বের মধ্যে রেখে দু'টি ভেদ্য সমান্তরাল প্রাচীরের গতি থেকে এই সমীকরণ-গুলি নির্ণিত হয়েছে। বিচলন কৃৎকৌশলের সাহায্যে গতিবেগ, উষ্ণতা এবং গাঢ়তা বন্টন নির্ণয় করা হয়েছে। যাডুনায়েস্কি কৃৎকৌশলের সাহায্যে আনুমানিক ভূ-গোলকীয় ত্রুটির হিসাব করা হয়েছে। আপাত সান্দ্র গুণাংকের উর্ধ-সীমার কার্যফল, রেনল্ডস্ সংখ্যা, ফর্স্ছিমার সংখ্যা, চুম্বকশীলতা প্রাচল, চাপ - নতির অপরিবর্তী উপাংশ, স্পন্দনের বিস্তার, প্রাণ্ড্ল সংখ্যা, একার্ট সংখ্যা, স্মিড্ সংখ্যা, সরেট সংখ্যা এবং গতিবেগ, উষ্ণতা এবং গাঢ়তা বন্টনের উপর কতটা সময় লেগে-ছিল তা নির্ণয় করা হয়েছে এবং লেখচিত্রে চিত্রিত করা হয়েছে।

1. Introduction

The problems of pulsatile flow have gained importance due to their immediate practical applications in biomechanical and engineering sciences. In physiology, pulsatile mechanism is involved in urine transport from kidney to bladder through the ureter, movement of chyme in the gastrointestinal tract, transport of spermatozoa in the ductus efferentes of the male reproductive tracts, and in the cervical canal, in movement of ovum in the fallopian tube, transport of lymph in the lymphatic vessels.

In situations like travel in vehicles, aircraft, operating jackammer and sudden movements of body during sports activities, the human body experiences external body acceleration. Prolonged exposure of a healthy human body to external acceleration may cause serious health problem like headache, increase of pulse rate and loss of vision on account of disturbances in blood flow [1].

The analysis of the mechanisms responsible for pulsatile transport have been studied by many authors. The problem of pulsatile flow with reference to stenosis in microcirculation was analysed by Bitoun and Bellet [2]. Rao and Rathna Devanathan [3] and Schneck and Ostrack [4] studied pulsatile flow through circular tubes of varying cross-section at low Reynolds number. In these studies the tube wall is taken to be impermeable. Macey [5, 6] studied the steady flow of a viscous fluid through a circular tube with a permeable wall. Radhakrishnamacharya et al. [7] extended this study to the flow through circular tubes of varying cross-section and permeable wall. Eldabe et al. [8,9] studied pulsatile magnetohydrodynamic viscoelastic flow through a channel bounded by two permeable parallel plates with the effect of couple stresses on pulsatile hydromagnetic Poiseuille flow. Many authors have studied the effect of porous medium on the motion of the fluid. Some of these studies have been made by Varshney [10], Raptis et al. [11,12], Raptis and Peridikis [13], Elshehawey et al. [14]. Flow through porous media is very prevalent in nature and therefore the study of flow through a porous medium has become of principle interest in many engineering applications. Thermal and solutal transport by fluid flowing through a porous matrix is phenomenon of great interest from the theory and application point of view. Heat transfer in the case of homogenous fluid-saturated porous media has been studied with relation of different applications like dynamic of hot underground springs, terrestrial heat flow through aquifer, hot fluid and ignition front displacements in reservoir engineering, heat exchange between soil and atmosphere and heat exchanges with fluidized beds. Mass transfer in isothermal condition has been studied with applications to problems of mixing of fresh and salt water in a quifers, spreading of solutes in fluidized beds and crystal washers, salt leaching in soils, etc. Prevention of salt dissolution into the lake water near the sea shores has become a serious problem of research [15].

In this paper, the main aim is to obtain a numerical solution of the problem of unsteady magneto-hydrodynamic pulsatile flow with heat and mass transfer. The fluid used is biviscosity fluid through a uniform porous media between two permeable parallel plates. The governing equations are solved by making use of Runge-Kutta-Merson method in a shooting and matching technique and we calculate the global error by using Zadunaisky technique [16]. We evaluate the influence of upper limit of apparent viscosity coefficient β, Reynolds number Re, the permeability parameter k, Forschheimer number Fs, the steady component of the pressure gradient Ps, the amplitude of the pulsation P_0, magnetic parameter M, Prandtl number Pr, Eckert number Ec, Schmidt number Sc and Soret number Sr on the different variables.

2. Mathematical analysis

We consider the unsteady flow with heat and mass transfer of a viscous, incompressible, and electrically conducting non-Newtonian fluid (biviscosity fluid) in a porous medium between two permeable parallel plates situated at $y = 0$ and h, under the action of the fluid gradient. The coordinates system used is given in Fig. 1. The x- axis is taken in the direction of the flow and the y- axis is taken normal to the plates. We assume that a uniform magnetic field B_0 acting along y- axis. The fluid is being

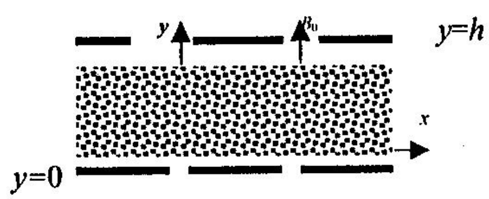

Fig. 1. Schematic of the problem

injected into the wall through $y = 0$ and is being sucked through $y = h$ with uniform velocity V_0.

The governing equations used in this problem can be written in normal tensorial notation as following (repeated indices are assumed over (i,j =1,3) unless otherwise stated).

Continuity equation:

$$\frac{d\rho}{dt} + \rho V_{i,i} = 0, \tag{1}$$

Momentum equation:

$$\frac{dV_i}{dt} = -\frac{1}{\rho}\frac{\partial P}{\partial x_i} + \frac{1}{\rho}\frac{\partial \tau_{ij}}{\partial x_j} + \frac{1}{\rho} \in_{ijk} J_j B_k + \frac{\nu}{\rho} V_i - b\sqrt{V_j V_j}\, V_i\,, \tag{2}$$

Temperature equation:

$$\frac{dT}{dt} = k_T \nabla^2 T + \frac{1}{\rho_c}\tau_{ij}\frac{\partial v_i}{\partial x_j}\,, \tag{3}$$

Concentration equation:

$$\frac{dC}{dt} = D\nabla^2 C + D\frac{k_T}{T_m}\nabla^2 T\,, \tag{4}$$

where V_i and τ_{ij} are the velocity and stress components, T and C are the temperature and concentration distributions, P and ρ are the fluid pressure and density of the fluid, J_j and B_k are the current density and intensity of magnetic induction, $\frac{d}{dt}$ denotes differentiation with respect to time following the material particle and $\in_{ijk}$, b, ν, c, k_T, D and T_m are the permutation symbol, Forchhemer's constant, kinematic viscosity, specific heat, thermal diffusion ratio, coefficient of mass diffusivity and mean fluid temperature.

We choose the biviscosity model [17] to describe the non-Newtonian fluid, which is in the usual notation

$$\tau_{ij} = \begin{cases} 2\left(\mu_B + \dfrac{p_y}{\sqrt{2\pi}}\right)e_{ij}, & \pi > \pi_c \\ 2\left(\mu_B + \dfrac{p_y}{\sqrt{2\pi_c}}\right)e_{ij}, & \pi < \pi_c. \end{cases} \tag{5}$$

The following quantity is introduced as a non dimensional parameter including π_c.

$$\beta = \mu_B \frac{\sqrt{2\pi}}{p_y},$$

where μ_B is the plastic viscosity, p_y is the yielding stress, $\pi = e_{ij}\, e_{ij}$, which e_{ij} is the (i,j) component of the deformation rate and the value of β denotes the upper limit of apparent viscosity coefficient. For ordinary Newtonian fluid $p_y = 0$.

Since the two walls are infinite in extent, all quantities are functions of y and t only, $\underline{V}=(U,V,0)$, $\underline{B}=(0,B_0,0)$. From equation (1) we get $V=V_0$ which is the velocity of the suction or injection at the walls. Equations (2), (3) and (4) reduce to

$$\frac{\partial u}{\partial t}+V_0\frac{\partial u}{\partial y}+\frac{1}{\rho}\frac{\partial P}{\partial x}=\nu_B(1+\beta^{-1})\frac{\partial^2 u}{\partial y^2}-\frac{\sigma B_0^2}{\rho}u-\frac{\nu}{k}u-bu^2, \tag{6}$$

$$\frac{\partial T}{\partial t}+V_0\frac{\partial T}{\partial y}=k_T\frac{\partial^2 T}{\partial y^2}+\frac{\nu_B}{c}(1+\beta^{-1})\left(\frac{\partial u}{\partial y}\right)^2, \tag{7}$$

$$\frac{\partial C}{\partial t}+V_0\frac{\partial C}{\partial y}=D\frac{\partial^2 C}{\partial y^2}+D\frac{k_T}{T_m}\frac{\partial^2 T}{\partial y^2}, \tag{8}$$

where σ is the electric conductivity. The appropriate boundary conditions are

$$u=0,\quad T=T_1\quad \text{and}\quad C=C_1\quad \text{at}\quad y=0, \tag{9}$$
$$u=0,\quad T=T_2\quad \text{and}\quad C=C_2\quad \text{at}\quad y=h, \tag{10}$$

where h is the distance between the two plates.

Let us introduce the dimensionless quantities as follows:

$$\left.\begin{aligned}&u^*=\frac{u}{V_0},\ x^*=\frac{1}{h}x,\ y^*=\frac{1}{h}y,\ w^*=\frac{h}{V_0}w,\ t^*=\frac{V_0}{h}t,\\&P^*=\frac{1}{\rho V_0^2}P,\ T^*=\frac{T-T_2}{T_1-T_2},\ C^*=\frac{C-C_2}{C_1-C_2},\end{aligned}\right\} \tag{11}$$

After substituting from equation (11), eqs. (6), (7) and (8) may be written in dimensionless form after dropping star mark.

$$\frac{\partial u}{\partial t}+\frac{\partial u}{\partial y}+\frac{\partial P}{\partial x}=\frac{1}{\mathrm{Re}}(1+\beta^{-1})\frac{\partial^2 u}{\partial y^2}-\left(M+\frac{1}{k}\right)u-F_s u^2, \tag{12}$$

$$\frac{\partial T}{\partial t}+\frac{\partial T}{\partial y}=\frac{1}{R_e P_r}\frac{\partial^2 T}{\partial y^2}+\frac{Ec}{R_e}(1+\beta^{-1})\left(\frac{\partial u}{\partial y}\right)^2, \tag{13}$$

$$\frac{\partial C}{\partial t}+\frac{\partial C}{\partial y}=\frac{1}{S_c}\frac{\partial^2 C}{\partial y^2}+S_r\frac{\partial^2 T}{\partial y^2}, \tag{14}$$

where $R_e=\dfrac{hV_0}{\nu_B}$ (the Reynolds number), $M=\dfrac{\sigma B_0^2 h}{\rho V_0}$ (the magnetic field parameter),

$k=\dfrac{kV_0}{\nu h}$ (the porosity parameter), $F_s=hb$ (Forschheimer number),

$P_r=\dfrac{\nu_B}{k_T}$ (Prandtl number), $Ec=\dfrac{V_0^2}{c(T_1-T_2)}$ (Eckert number),

$S_c=\dfrac{hV_0}{D}$ (Schmidt number) and $S_r=\dfrac{Dk_T(T_1-T_2)}{hT_m V_0(C_1-C_2)}$ (Soret number). (15)

For pulsation pressure gradient, let

$$-\frac{\partial P}{\partial x}=\left(\frac{\partial P}{\partial x}\right)_s+\left(\frac{\partial P}{\partial x}\right)_0 e^{i\omega t}, \tag{16}$$

The equations (12), (13) and (14) can be solved by using the following perturbation technique:

$$\left.\begin{aligned} u&=u_s+u_0e^{i\omega t},\\ T&=T_s+T_0e^{i\omega t},\\ C&=C_s+C_0e^{i\omega t}\end{aligned}\right\}. \tag{17}$$

Substituting from (16) and (17) in (12), (13) and (14) and equating the like terms on both sides, we get the following system equations:

$$-\frac{1}{R_e}(1+\beta^{-1})\frac{d^2u_s}{dy^2}+\left(M+\frac{1}{k}\right)u_s+\frac{du_s}{dy}+F_su_s^2=\left(\frac{\partial P}{\partial x}\right)_s, \tag{18}$$

$$-\frac{1}{R_e}(1+\beta^{-1})\frac{d^2u_0}{dy^2}+\left(M+\frac{1}{k}+i\omega\right)u_0+\frac{du_0}{dy}+2F_su_su_0=\left(\frac{\partial P}{\partial x}\right)_0, \tag{19}$$

$$\frac{1}{R_eP_r}\frac{d^2T_s}{dy^2}+\frac{E}{R_e}(1+\beta^{-1})\left(\frac{du_s}{dy}\right)^2-\frac{dT_s}{dy}=0, \tag{20}$$

$$\frac{1}{R_eP_r}\frac{d^2T_0}{dy^2}+\frac{2E}{R_e}(1+\beta^{-1})\left(\frac{du_s}{dy}\right)\left(\frac{du_0}{dy}\right)-\frac{dT_0}{dy}-i\omega T_0=0, \tag{21}$$

$$\frac{1}{S_c}\frac{d^2C_s}{dy^2}+S_r\frac{d^2T_s}{dy^2}-\frac{dC_s}{dy}=0, \tag{22}$$

$$\frac{1}{S_c}\frac{d^2C_0}{dy^2}+S_r\frac{d^2T_0}{dy^2}-\frac{dC_0}{dy}-i\omega C_0=0. \tag{23}$$

The dimensionless boundary conditions are

$$\left.\begin{array}{ll} u_s=0,\ u_0=0,\ T_s=1,\ T_0=0,\ C_s=1,\ C_0=0 & \text{at } y=0 \\ u_s=0,\ u_0=0,\ T_s=T_0=0,\ C_s=C_0=0 & \text{at } y=1 \end{array}\right\}. \tag{24}$$

We assume the complex variables u_0, T_0 and C_0 as follows:

$$\left.\begin{array}{l} u_0=u_{01}+i\omega u_{02}, \\ T_0=T_{01}+i\omega T_{02}, \\ C_0=C_{01}+i\omega C_{02} \end{array}\right\}. \tag{25}$$

Equations (19), (21) and (23) reduce to the following system of equations after comparing the real and imaginary parts

$$-\frac{1}{R_e}(1+\beta^{-1})\frac{d^2u_{01}}{dy^2}+\left(M+\frac{1}{k}\right)u_{01}+\frac{du_{01}}{dy}+2F_su_su_{01}-\omega^2u_{02}=\left(\frac{\partial P}{\partial x}\right)_0, \tag{26}$$

$$-\frac{1}{R_e}(1+\beta^{-1})\frac{d^2u_{02}}{dy^2}+\left(M+\frac{1}{k}\right)u_{02}+u_{01}+\frac{du_{02}}{dy}+2F_su_su_{02}=0, \tag{27}$$

$$\frac{1}{R_eP_r}\frac{d^2T_{01}}{dy^2}+\frac{2E}{R_e}(1+\beta^{-1})\left(\frac{du_s}{dy}\right)\left(\frac{du_{01}}{dy}\right)-\frac{dT_{01}}{dy}+\omega^2T_{02}=0, \tag{28}$$

$$\frac{1}{R_eP_r}\frac{d^2T_{02}}{dy^2}+\frac{2E}{R_e}(1+\beta^{-1})\left(\frac{du_s}{dy}\right)\left(\frac{du_{02}}{dy}\right)-\frac{dT_{02}}{dy^2}-T_{01}=0, \tag{29}$$

$$\frac{1}{S_c}\frac{d^2C_{01}}{dy^2}+S_r\frac{d^2T_{01}}{dy^2}-\frac{dC_{01}}{dy}+\omega^2C_{02}=0, \tag{30}$$

$$\frac{1}{S_c}\frac{d^2C_{02}}{dy^2}+S_r\frac{d^2T_{02}}{dy^2}-\frac{dC_{02}}{dy}-C_{01}=0, \tag{31}$$

and hence the boundary conditions (24) transform into

$$\left.\begin{array}{ll} u_s=0,\ u_{01}=u_{02}=0,\ T_s=1,\ T_{01}=T_{02}=0,\ C_s=1,\ C_{01}=C_{02}=0 & \text{at } y=0 \\ u_s=0,\ u_{01}=u_{02}=0,\ T_s=T_{01}=T_{01}=0,\ C_s=C_{01}=C_{02}=0 & \text{at } y=1 \end{array}\right\}. \tag{32}$$

3. Numerical treatment

Let

$u_s=Y_1$, $u_{01}=Y_3$, $u_{02}=Y_5$, $T_s=Y_7$, $T_{01}=Y_9$, $T_{02}=Y_{11}$, $C_s=Y_{13}$, $C_{01}=Y_{15}$ and $C_{02}=Y_{17}$.

Hence equations (18), (20), (22) and (26-31) can be written as follows:

$$\left.\begin{aligned}
&Y_1'=Y_2, Y_2'=\frac{R_e}{(1+\beta^{-1})}\left[Y_2+\left(M+\frac{1}{k}\right)Y_1+F_sY_1^2-P_S,\right],\\
&Y_3'=Y_4, Y_4'=\frac{R_e}{(1+\beta^{-1})}\left[Y_4+\left(M+\frac{1}{k}\right)Y_3+2F_sY_1Y_3-\omega^2Y_5-P_0,\right],\\
&Y_5'=Y_6, Y_6'=\frac{R_e}{(1+\beta^{-1})}\left[Y_6+\left(M+\frac{1}{k}\right)Y_5+2F_sY_1Y_5+Y_3\right],\\
&Y_7'=Y_8, Y_8'=R_e\Pr Y_8-E\Pr(1+\beta^{-1})Y_2^2,\\
&Y_9'=y_{10}, Y_{10}'=R_e\Pr(Y_{10}-\omega^2Y_{11})-2E\Pr(1+\beta^{-1})Y_2Y_4,\\
&Y_{11}'=Y_{12}, Y_{12}'=R_e\Pr(Y_9+Y_{12})-2E\Pr(1+\beta^{-1})Y_2Y_6,\\
&Y_{13}'=Y_{14}, Y_{14}'=-S_cS_r(R_e\Pr Y_8-E\Pr(1+\beta^{-1})Y_2^2)+S_cY_{14},\\
&Y_{15}'=Y_{16},\\
&Y_{16}'=-S_cS_r(R_e\Pr(Y_{10}-\omega^2Y_{11})-2E\Pr(1+\beta^{-1})Y_2Y_4)+S_c(Y_{16}-\omega^2Y_{17}),\\
&Y_{17}'=Y_{18}, Y_{18}'=-S_cS_r(R_e\Pr(Y_9+Y_{12})-2E\Pr(1+\beta^{-1})Y_2Y_6)+S_c(Y_{18}+Y_{15}),
\end{aligned}\right\}, \quad (33)$$

where prime denotes to differentiation with respect to y and this system (33) subject to the boundary conditions

$$\left.\begin{aligned}
&Y_1=0,\ Y_3=Y_5=0,\ Y_7=1,\ Y_9=Y_{11}=0,\ Y_{13}=1,\ Y_{15}=Y_{17}=0 \quad \text{at} \quad y=0\\
&Y_1=0,\ Y_3=Y_5=0,\ Y_7=Y_9=Y_{11}=0,\ Y_{13}=Y_{15}=Y_{17}=0 \quad \text{at} \quad y=1
\end{aligned}\right\}. \quad (34)$$

To apply shooting method we use the subroutine D02HAF from the NAG Fortran library, which requires the supply of starting values of the missing initial and terminal conditions. The subroutine uses Runge-Kutta-Merson method with variable step size in order to control the local truncation error, then it applies modified Newton-Raphson technique mentioned before to make successive corrections to the estimated boundary values. The process is repeated iteratively until convergence is obtained i.e. until the absolute values of the difference between every two successive approximations of the missing conditions is less than ε (in our case ε is taken = 10^{-7}).

4. Estimation of the global error

We use Zadunaisky technique [16] to calculate the global error, which can be explained in the following steps:

1.We interpolate the functions of Y_I (I=1,2,...,18) from the values of Y_I and we named them P_I (I=1,2,.....,18), and we interpolate the functions of

$u''_s, u''_{01}, u''_{02}, T''_s, T''_{01}, T''_{02}, C_s, C''_{01}, C''_{02}$ and we named that $R_1(y) = u''_s, R_2(y) = u''_{01}$, $R_3(y) = u''_{02}, R_4(y) = T''_s, R_5(y) = T''_{01}, R_6(y) = T''_{02}, R_7(y) = C_s, R_8(y) = C''_{01}, R_9(y) = C''_{02}$

2. We calculate the detect functions D_l (l=1,2,...,18), which can be written as follows:

$$D_1(y)= P'_1 - P_2 =0,\quad D_2(y)= P'_2 - R_1(y),\quad D_3(y)= P'_3 - P_4 =0,$$

$$D_4(y)= P'_4 - R_2(y),\quad D_5(y)= P'_5 - P_6 =0,\quad D_6(y)= P'_6 - R_3(y),$$

$$D_7(y)= P'_7 - P_8 =0,\quad D_8(y)= P'_8 - R_4(y),\quad D_9(y)= P'_9 - P_{10} =0,$$

$$D_{10}(y)= P'_{10} - R_5(y),\quad D_{11}(y)= P'_{11} - P_{12} =0,\quad D_{12}(y)= P'_{12} - R_6(y),$$

$$D_{13}(y)= P'_{13} - P_{14} =0,\quad D_{14}(y)= P'_{14} - R_7(y),\quad D_{15}(y)= P'_{15} - P_{16} =0,$$

$$D_{16}(y)= P'_{16} - R_8(y),\quad D_{17}(y)= P'_{17} - P_{18} =0,\quad D_{18}(y)= P'_{18} - R_9(y). \qquad (35)$$

3. We add the detect functions D_l (l=1,2,...,18) to the original problem (33) and change every Y_l with another variable Z_l (l=1,2,...,18).

4. We solved the pseudo problem by the same method and we will have the solution $\underline{Z}(y)$ whose elements Z_l (l=1,2,...,18).

5. We calculate the global error from the relation $e_n = \underline{Z}_n - \underline{Z}(y_n) = \underline{Z}_n - \underline{P}(y_n)$, (n=1,2,...,6), where $\underline{Z}_n$ is the approximated solution of the pseudo problem at the point y_n and $\underline{Z}(y_n)$ is the exact solution of the pseudo problem at y_n.

Obviously the exact solution of original problem (33) is

$$\underline{Z}(y_n) = \underline{P}(y_n).$$

The values of the global error are shown in table (1). This error is based on using 6 points to find the interpolation polynomials P_l (l=1,2,...,18), of degree 5.

In order to achieve the above task we used combination of programs in Fortran (using NAG library routine D02HAF) and Mathematica package.

y	$u_s=y_1$	error(e1)	$T_s=y_7$	error(e7)	$C_s=y_{13}$	error(e13)
0	.000D+00	.000D+00	1	.000D+00	1	.000D+00
0.2	.361D-01	.000D+00	.810 D+00	.000D+00	.812 D+00	.000D+00
0.4	.518D-01	.000D+00	.614 D+00	.000D+00	.618 D+00	.000D+00
0.6	.520D-01	.000D+00	.414 D+00	.000D+00	.418 D+00	.000D+00
0.8	.365D-01	.000D+00	.21 D+00	.000D+00	.212 D+00	.000D+00
1	.000D+00	.555D-05	.000D+00	.822D-06	.000D+00	.504D-07

Table (1).

5. Numerical results and discussion

Our aim in this research is to study the MHD pulsatile flow with heat and mass transfer of non-Newtonian fluid (biviscosity fluid) in a porous medium between two permeable parallel plates. The equations of momentum, energy and concentration have been solved by using perturbation technique. A Rung-Kutta-Merson method and a Newtonian iteration in a shooting and matching technique are used to solve the nonlinear differential equations. The velocity, temperature and concentration distributions are calculated for different values of upper limit of apparent viscosity coefficient β, Reynolds number R_e, the magnetic parameter M, the porous parameter k, Forschheimer number Fs, the steady component of the pressure gradient Ps, the amplitude of the pulsation P_0, Prandtl number Pr, Eckert number Ec, Schmidt number Sc, Soret number Sr, and the time.

The effects of physical parameters on the velocity distribution are indicated through figures (2-9). In these figures the velocity distribution u is potted versus the coordinate y. Figs. (2) and (3) illustrate the effects of upper limit of apparent viscosity coefficient β and Reynolds number R_e. It is found that the velocity increases with increasing both β and R_e. the effect of the magnetic parameter M on the velocity is to decrease it which is clearly depicted in figure 4. Figures (5), (6) and (7) are plotted to elucidate the influences of the porous parameter k, the steady component of the pressure gradient Ps and the amplitude of the pulsation P_0 on the velocity. It is observed that as k, Ps and P_0 increase the velocity increases. The influences of Forschheimer number Fs and the time t on the velocity are illustrated in figures (8) and (9). Increasing Fs and t have a tendency to decrease the velocity.

The effects of different parameters on the temperature distribution T are indicated graphically through figures (10-17). In figures (10), (11) and (12), we observe that the temperature distribution T decreases with the increase of the magnetic parameter M, Forschheimer number Fs and the time t. The effects of upper limit of apparent viscosity coefficient β, Reynolds number R_e, porous parameter k, Prandtl number Pr and Eckert number Ec on the temperature distribution T are elucidated in figures (13), (14), (15), (16) and (17). It is seen that T increases as β, R_e, k, Pr and Ec increase

Figures (18-25) are graphed to illustrate the effects of the physical parameters on the concentration distribution C. The concentration is plotted versus y for various values of β, R_e, k and Schmidt number Sc in figures (18), (19), (20) and (21). It is found that C increase with the increase of β, R_e, k and Sc. The effect of M, Fs, t and Soret number Sr in figures (22), (23), (24) and (25). It is indi.cated that as M, Fs, t and Sr increase C decreases.

Fig. 2. Velocity distribution plotted against position for t=π/2, Re=.1, M=1, K=.01, Ps=10, P0=7, Pr=1, E=2, Sc=.15, Sr=.05, Fs=10, w=1.

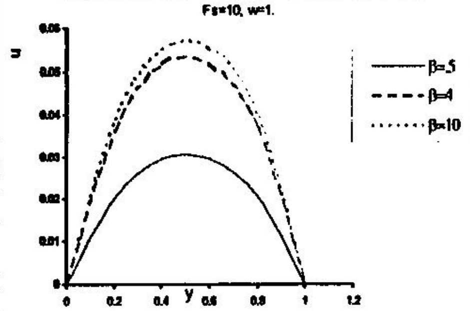

Fig. 3. Velocity distribution plotted against position for t=π/2, β=4, M=1, K=.01, Ps=10, P0=7, Pr=1, E=2, Sc=.15, Sr=.05, Fs=10, w=1.

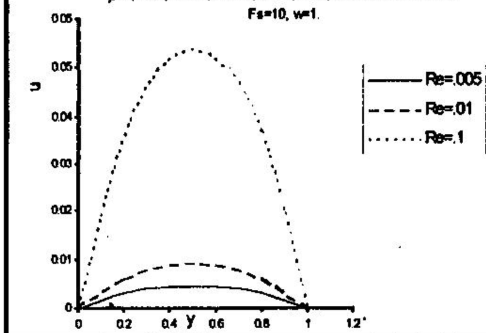

Fig. 4. Velocity distribution plotted against position for t=π/2, b=4, Re=.1, K=.01, Ps=10, P0=7, Pr=1, E=2, Sc=.15, Sr=.05, Fs=10, w=1.

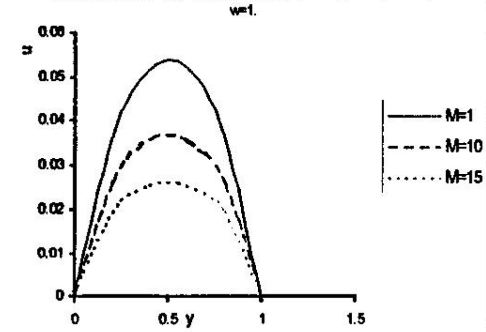

Fig. 5. Velocity distribution plotted against position for t=π/2, b=4, Re=.1, M=1, Ps=10, P0=7, Pr=1, E=2, Sc=.15, Sr=.05, Fs=10, w=1.

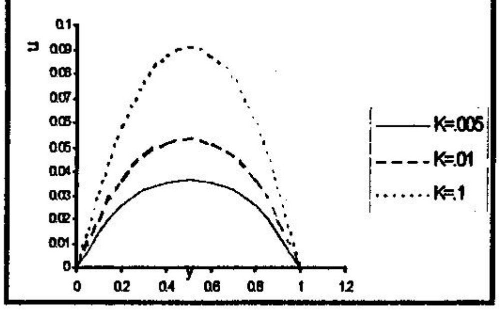

Fig. 6. Velocity distribution plotted against position for t=π/2, b=4, Re=.1, M=1, K=.01, P0=7, Pr=1, E=2, Sc=.15, Sr=.05, Fs=10, w=1.

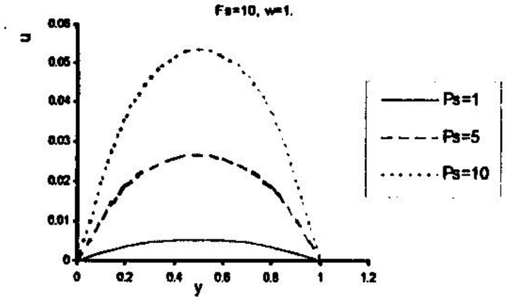

Fig. 7. Velocity distribution plotted against position for t=π/2, β=4, Re=.1, M=1, K=.01, Ps=10, Pr=1, E=2, Sc=.15, Sr=.05, Fs=10, w=1, t=0.

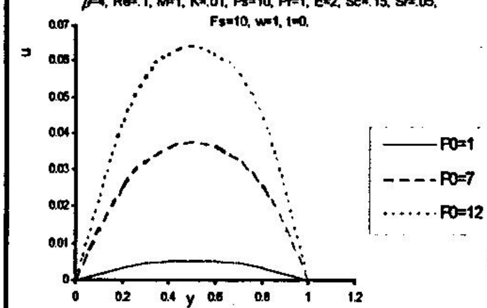

Fig. 8. Velocity distribution plotted against position for $t=\pi/2$, $\beta=4$, Re=.1, M=1, K=.01, Ps=10, P0=7, Pr=1, E=2, Sc=.15, Sr=.05, w=1.

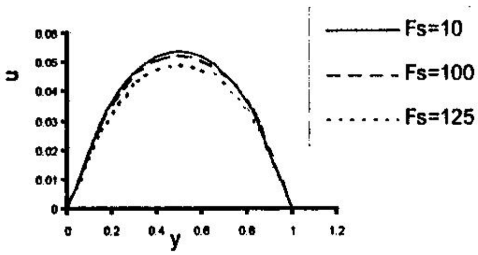

Fig. 9. Velocity distribution plotted against position for $\beta=4$, Re=.1, M=1, K=.01, Ps=10, P0=7, Pr=1, E=2, Sc=.15, Sr=.05, Fs=10, w=1.

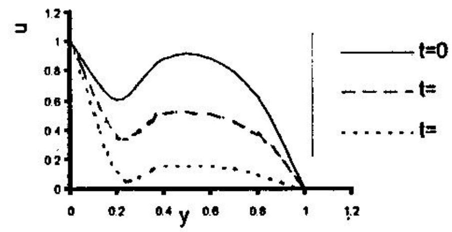

Fig. 11. Temperature distribution plotted against position for t=0, $\beta=4$, Re=.1, M=1, K=.01, Ps=10, P0=7, Pr=1, E=2, Sc=.15, Sr=.05, w=1.

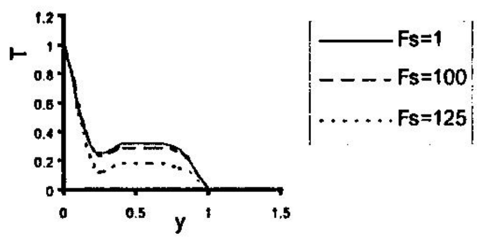

Fig. 10. Temperature distribution plotted against position for t=0, $\beta=4$, Re=.1, K=.01, Ps=10, P0=7, Pr=1, E=2, Sc=.15, Sr=.05, Fs=10, w=1.

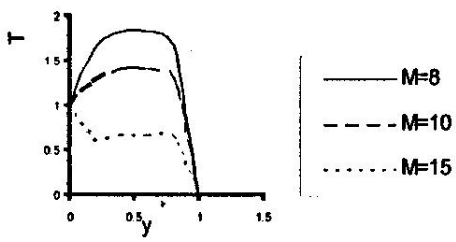

Fig. 12. Temperature distribution plotted against position for $\beta=4$, Re=.1, M=1, K=.01, Ps=10, P0=7, Pr=1, E=2, Sc=.15, Sr=.05, Fs=10, w=1.

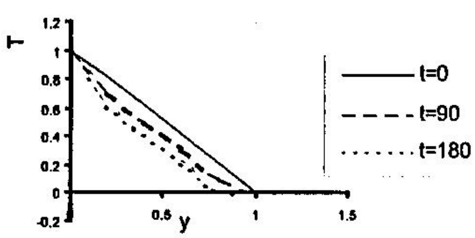

Fig. 13. Temperature distribution plotted against position for t=0, Re=.1, M=1, K=.01, Ps=10, P0=7, Pr=1, E=2, Sc=.15, Sr=.05, Fs=10, w=1.

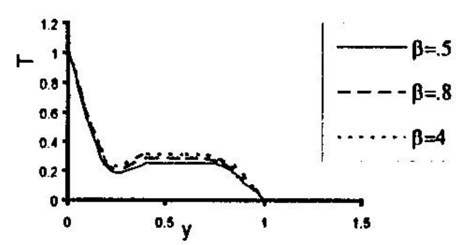

Fig. 14. Temperature distribution plotted against position for t=0, $\beta=4$, M=1, K=.01, Ps=10, P0=7, Pr=1, E=2, Sc=.15, Sr=.05, Fs=10, w=1.

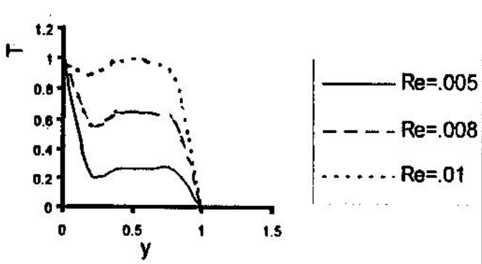

Fig. 15. Temperature distribution plotted against position for t=0, $\beta=4$, Re=.1, M=1, Ps=10, P0=7, Pr=1, E=2, Sc=.15, Sr=.05, Fs=10, w=1.

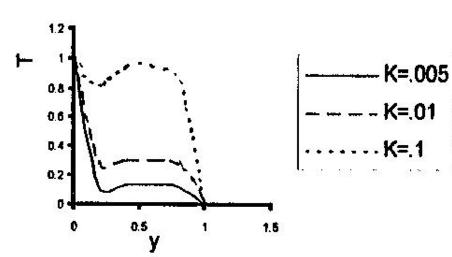

Fig. 16. Temperature distribution plotted against position for $t=\pi/2$, $\beta=4$, Re=.1, M=1, K=.01, Ps=10, P0=7, E=2, Sc=.15, Sr=.05, Fs=10, w=1.

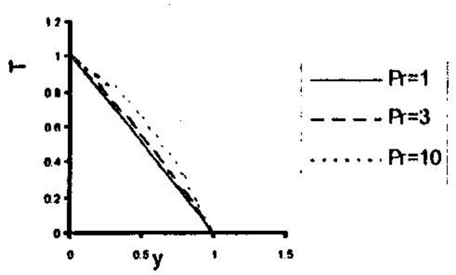

Fig. 17. Temperature distribution plotted against position for $t=\pi/2$, $\beta=4$, Re=.1, M=1, K=.01, Ps=10, P0=7, Sc=.15, Sr=.05, Fs=10, w=1.

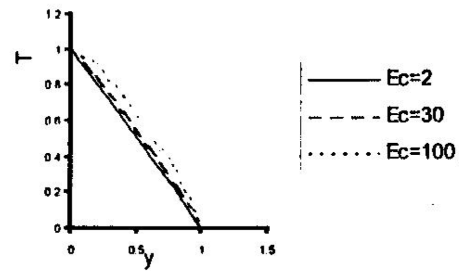

Fig. 18. Concentration distribution plotted against position for t=0, Re=.1, M=1, K=.01, Ps=10, P0=7, Pr=1, E=2, Sc=.15, Sr=.05, Fs=10, w=1.

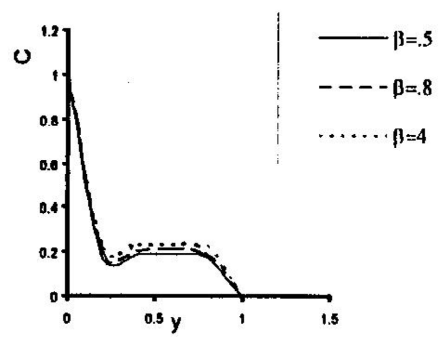

Fig. 19. Concentration distribution plotted against position for t=0, $\beta=4$, M=1, K=.01, Ps=10, P0=7, Pr=1, E=2, Sc=.15, Sr=.05, Fs=10, w=1.

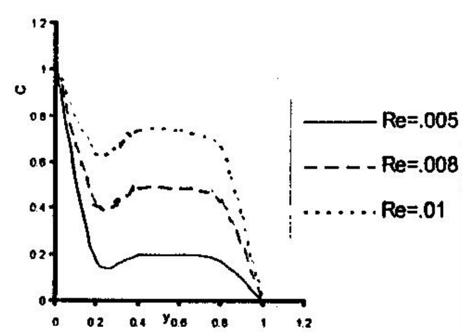

Fig. 20. Concentration distribution plotted against position for t=0, $\beta=4$, Re=.1, M=1, Ps=10, P0=7, Pr=1, E=2, Sc=.15, Sr=.05, Fs=10, w=1.

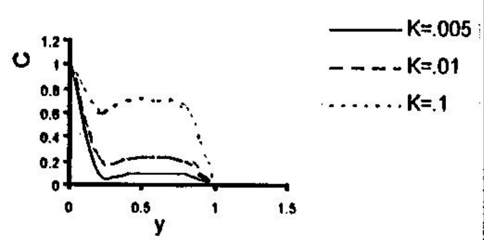

Fig. 21. Concentration distribution plotted against position for $t=\pi/2$, $\beta=4$, Re=.1, M=1, K=.01, Ps=10, P0=7, Pr=1, E=2, Sr=.05, Fs=10, w=1.

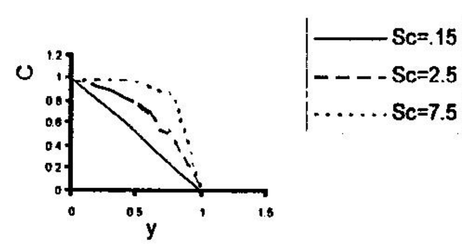

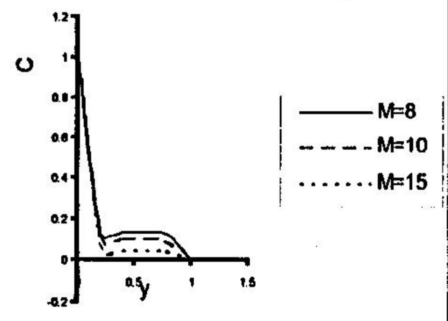

Fig. 22. Conentration distribution plotted against position for t=0, β=4, Re=.1, K=.01, Ps=10, P0=7, Pr=1, E=2, Sc=.15, Sr=.05, Fs=10, w=1.

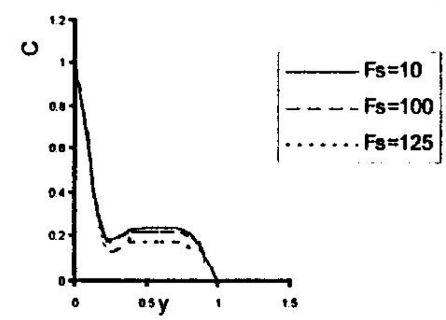

Fig. 23. Concentration distribution plotted against position for t=0, β=4, Re=.1, M=1, K=.01, Ps=10, P0=7, Pr=1, E=2, Sc=.15, Sr=.05, w=1.

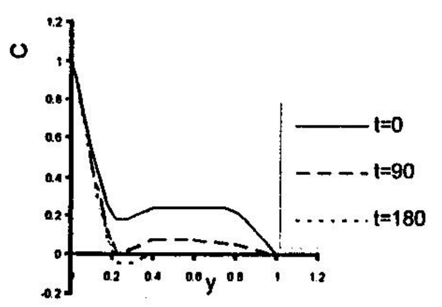

Fig. 24. Concentration distribution plotted against position for β=4, Re=.1, M=1, K=.01, Ps=10, P0=7, Pr=1, E=2, Sc=.15, Sr=.05, Fs=10, w=1.

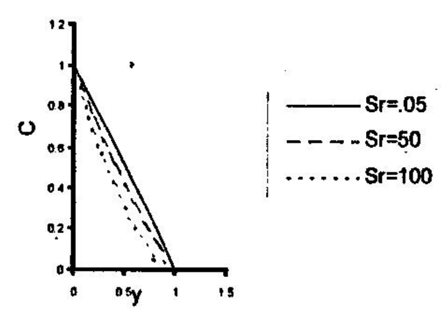

Fig. 25. Concentration distribution plotted against position for t=π/2, β=4, Re=.1, M=1, K=.01, Ps=10, P0=7, Pr=1, E=2, Sc=.15, Fs=10, w=1.

6. Conclusion

In this paper, we have studied the problem of unsteady flow with heat and mass transfer of non-Newtonian fluid (biviscosity fluid) through a uniform porous medium between two permeable parallel plates in the presence of magnetic field. The equations of momentum, energy and concentration are solved by using the perturbation technique. The governing equations were solved by using Rung-Kutta-Merson method and Newton iteration in shooting and matching technique. Also, we obtain an estimation of the error propagation by using Zadunaisky technique. The errors estimated justify the use of the approximated solutions as a suitable approximation to the calculated physical values. Numerical calculations are presented for the velocity, the fluid temperature, fluid concentration and their dependence on the material parameters of the fluid. The effects of these parameters are discussed by a set of graphs. It was found that increases in any of the following: Reynolds number and the porous parameter caused increment in the velocity, temperature, concentration distributions and inversely increases in the magnetic parameter, Forschheimer number and the time caused reduction in the same distributions.

References

1) S.N Majhi and V.R Nair,: *Int. J. Eng. Sci.* **32** (1994), 839-846.
2) J.P. Bitoun and D. Bellet: *Biorheology* **23** (1986), 51.
3) Ramachandra Rao and Rathna Devanathan: *Z. A. M. P.* **24** (1973), 203.
4) D. J. Schneck and S. Ostrach: J. *Fluids Eng.* **16** (1975), 353.
5) R. I. Macey: *Bull. Math. Biophys.* **25** (1963), 1.
6) R. I. Macey: *Bull. Math. Biophys.* **27** (1965), 117.
7) G. Radhakrishnamacharya, Peeyush Chandra and M. R. Kaimal: *Bull. Math. Biol.* **43** (1981), 151.
8) Nabil T. M. Eldabe and Salwa M. G. Elmohandis: . *Phys. Soc. Japan.* **64** (1995), 4165.
9) Nabil T. M. Eldabe and Salwa M. G. Elmohandis: *Fluid Dynamic Research.* **15** (1995), 313.
10) C. L. Varshney: *J. Pure Appl. Math.* **10** (1979), 1558.
11) Raptis, C. Peridikis and G. Tzivanidis: J. Phys. D: Appl. Phys. 14 (1981), L99.
12) Raptis, N. Kafousias and C. Massalas: *ZAMM* **62** (1982), 489.
13) Raptis and C. Peridikis: *Int. J. Engng. Sci.* **21** (1983), 1327.
14) Elsayed F. Elshehawey, Ayman M. F. Sobh and Elsayed M. E. Elbarbary: *J.Phys. Soc. Japan.* **69** (2000), 401.
15) S. N. Murthy, Tran: ASME *J. Heat Transfer,* **122** (2000), 476.
16) P. E Zadunaisky : *Numer. Math.* **27** (1976), 21.
17) M Nakayama and T Sawada : *J. Biomech. Eng.* **110** (1988), 137.